Smart Structures and Systems, *Vol. 19, No. 6 (2017) 695-703*
DOI: https://doi.org/10.12989/sss.2017.19.6.695

Electro-magneto-elastic analysis of a three-layer curved beam

Mohammad Arefi*[1] and Ashraf M. Zenkour[2,3a]

[1]*Department of Solid Mechanics, Faculty of Mechanical Engineering, University of Kashan, Kashan 87317-51167, Iran*
[2]*Department of Mathematics, Faculty of Science, King Abdulaziz University, Jeddah 21589, Saudi Arabia*
[3]*Department of Mathematics, Faculty of Science, Kafrelsheikh University, Kafrelsheikh 33516, Egypt*

(Received November 18, 2016, Revised April 26, 2017, Accepted April 29, 2017)

Abstract. In this paper, based on first-order shear deformation theory, the governing equations of motion for a sandwich curved beam including an elastic core and two piezo-magnetic face-sheets are presented. The curved beam model is resting on Pasternak's foundation and subjected to applied electric and magnetic potentials on the piezo-magnetic face-sheets and transverse loading. The five equations of motion are analytically solved and the bending and vibration results are obtained. The influence of important parameters of the model such as direct and shear parameters of foundation and applied electric and magnetic potentials are studied on the electro-mechanical responses of the problem. A comparison with literatures was performed to validate our formulation and results.

Keywords: three-layer curved beam; piezo-magnetic face-sheets; Pasternak's foundation; first-order shear deformation theory

1. Introduction

Studying the problem in various configurations and shapes needs more consideration and development of mathematical equations. For example analysis of the structures such as curved beams or doubly curved plates needs more complexities and mathematical operations rather than corresponding straight structures. Due to these conditions, analysis of straight structures have attracted more considerations from various researchers rather than curved or doubly curved structures. In this work, we focus on the combination of curved beam with multi-field loads and first-order shear deformation theory.

Vibration control of a composite beam integrated with curved piezoelectric layers was studied by Sun and Tong (2001) using a novel method for designing fiber modal sensors and modal actuators based on curved piezoelectric fiber. The influence of the curvatures of the fibers was investigated on the sensing signals. Sun and Tong (2002) presented a method for analysis of thin-walled curved beams with partially debonded piezoelectric actuator/sensor patches. They solved the problem using displacement continuity and force equilibrium conditions at the interfaces between the bonded and debonded regions. Shi (2005) analyzed bending behaviors of a piezoelectric and functionally graded curved actuator based on theory of piezo-elasticity subjected to an external voltage. The influence of power index of functionally graded material was investigated on the results and the obtained results were approved by comparison with finite element approach.

Koutsawa and Daya (2007) presented static and free vibration analyses of laminated glass beam rest on viscoelastic foundation. For free vibration analysis, finite element method was used. Kuang *et al*. (2007) investigated static responses of a circular curved beam bonded with piezoelectric actuators. The model was studied by one-dimensional beam theory of piezo-elasticity and the obtained results were verified by comparison with finite element results. The influence of electric potential on the bending analysis of a functionally graded piezoelectric curved beam was studied by Shi and Zhang (2008). Theory of piezo-elasticity was employed for derivation of the governing equations of the model and the bending results were derived using Taylor series expansion method. Electro-elastic analysis of piezoelectric laminated slightly curved beams was performed by Susanto (2009) based on an analytical model. The author has mentioned that stretching-bending coupling due to curvature has a considerable effect on the frequency parameters. The numerical results showed that increasing the radius of curvature leads to increase of the natural frequencies of curved beam.

Zhou *et al*. (2010) studied the transient analysis of a curved piezoelectric beam with variable curvature as piezoelectric vibration energy harvester. The influence of surface effects was studied on the electromechanical response of a curved piezoelectric nanobeam subjected to mechanical and electrical loads by Yan and Jiang (2011) based on Euler–Bernoulli curved beam theory. They mentioned some usefulness of the current model as nanoswitches or nanoactuators for control of displacement. Arefi (2014) studied piezo-magnetic analysis of a thick shell of revolution made of functionally graded materials using tensor analysis and a curvilinear coordinate system.

*Corresponding author, Dr.
E-mail: arefi63@gmail.com
[a] Professor
E-mail: zenkour@kau.edu.sa

ISSN: 1738-1584 (Print), 1738-1991 (Online)

Arslan and Usta (2014) employed theory of elasticity for electro-mechanical analysis of a curved bar. A comparison with previous results including an actuator under an initial electric potential was performed for verification of the results. The influence of the applied couple has been studied on the electro-mechanical results such displacement and electric potential distribution. Arefi and Khoshgoftar (2014) studied the influence of gradation of piezoelectric materials and electric potential on the electro-elastic analysis of a spherical shell. Arefi (2015) studied elastic solution of a curved beam made of functionally graded materials with various cross sections such as circular, rectangular and triangular. The influence of some important parameters such as non-homogeneous index and various cross sections was investigated on the stress distribution of curved beam. Hosseini and Rahmani (2016a) studied free vibration responses of curved functionally graded nanobeam based on nonlocal elasticity theory using Hamilton's principle. They presented an analytical approach based on Navier method to investigate the influence of parameter, opening angle, aspect ratio, mode number, and gradient index on the responses of curved nanobeam. Hosseini and Rahmani (2016b) presented an analytical approach for calculation of thermal buckling loads and natural frequencies of temperature dependent functionally graded curved beam. The influence of nonlocal parameter and temperature loads was investigated on the buckling loads and natural frequencies of nanobeam using nonlocal elasticity theory. They mentioned that considering temperature dependencies leads to lower natural frequency responses. Kananipour *et al.* (2014) developed differential quadrature method for dynamic analysis of a curved nanobeam.

Zhou *et al.* (2016) studied the piezoelectric laminated curved nanobeams with variable curvature as an element of electromechanical systems. They modeled the curved beam using radial and tangential displacements and rotation. The influence of some geometrical parameters and patterns of layers studied in detail. The influence of applied electric and magnetic potentials on the sandwich rod, beam and plates was studied by the first two authors (Arefi and Zenkour 2017, Arefi and Zenkour 2016 a, b, c, d, e Zenkour and Arefi 2017 a).

In this paper, the first-order shear deformation theory is used to derive the governing equations of motion for a sandwich curved beam integrated with piezomagnetic face-sheets. The electric and magnetic potentials is assumed as combination of a linear function along the thickness direction that reflects applied electric and magnetic potentials and a cosine function that reflects electric and magnetic boundary conditions. Combination of curved beam problem with piezo-magnetic materials leads to an important and novel subject that can be applicable in electro-mechanical systems as sensor and actuator for control of deflections or stresses.

2. Formulation

In this section, the formulation of a curved beam is presented. Two displacement components are considered including radial and circumferential displacements. First-order shear deformation theory is used for circumferential displacement. Based on this theory, two displacement components are expressed as (Arefi and Rahimi 2014, Arefi 2015, Shi and Zhang 2008)

$$\begin{aligned} u_r(r,\theta) &= u_r(\theta), \\ u_\theta(r,\theta) &= u_\theta(\theta) + \zeta\chi(\theta), \end{aligned} \tag{1}$$

in which $\zeta = r - R$. In addition, $u_r(\theta), u_\theta(\theta)$ are radial and circumferential displacements of mid-surface and $\chi(\theta)$ is beam rotation. In Eq. (1), ζ shows variation from mid-surface (Fig. 1).

Strain-displacement relations based on polar coordinate are defined as

$$\begin{aligned} \varepsilon_{rr} &= \frac{\partial u_r}{\partial r} = 0, \\ \varepsilon_{\theta\theta} &= \frac{u_r}{r} + \frac{1}{r}\frac{\partial u_\theta}{\partial \theta} = \frac{u_r}{R+\zeta} + \frac{1}{R+\zeta}\frac{\mathrm{d}u_\theta}{\mathrm{d}\theta} + \frac{\zeta}{R+\zeta}\frac{\mathrm{d}\chi}{\mathrm{d}\theta}, \\ \varepsilon_{r\theta} &= \frac{1}{r}\frac{\partial u_r}{\partial \theta} + \frac{\partial u_\theta}{\partial r} - \frac{u_\theta}{r} = \frac{1}{R+\zeta}\frac{\mathrm{d}u_r}{\mathrm{d}\theta} + \chi - \frac{u_\theta}{R+\zeta} - \frac{\zeta}{R+\zeta}\chi, \end{aligned} \tag{2}$$

In this stage, the stress components including circumferential and shear stresses for elastic core are defined as

$$\begin{aligned} \sigma^c_{\theta\theta} &= C^c_{\theta\theta\theta\theta}\varepsilon_{\theta\theta}, \\ \sigma^c_{r\theta} &= C^c_{r\theta r\theta}\varepsilon_{r\theta}, \end{aligned} \tag{3}$$

in which C^c_{ijkl} are stiffness coefficients of elastic core. The constitutive relations for piezomagnetic face-sheets are defined as (Arefi 2014, Arefi and Zenkour 2016 a, b, c, d, Shi and Zhang 2008)

$$\begin{aligned} \sigma^p_{\theta\theta} &= C^p_{\theta\theta\theta\theta}\varepsilon_{\theta\theta} - e^p_{\theta\theta r}E_r - q^p_{\theta\theta r}H_r, \\ \sigma^p_{r\theta} &= C^p_{r\theta r\theta}\varepsilon_{r\theta} - e^p_{r\theta\theta}E_\theta - q^p_{r\theta\theta}H_\theta, \end{aligned} \tag{4}$$

in which C^p_{ijkl} are stiffness coefficients of elastic core. In addition, e^p_{ijk} are the piezoelectric coefficients, q^p_{ijk} are piezomagnetic coefficients, E_i and H_i are the components of electric and magnetic fields, respectively. For calculation of stress in piezo-magnetic face-sheets, it is necessary to calculate electric and magnetic fields. Electric and magnetic fields are derived using electric and magnetic potentials as (Arefi and Zenkour 2016 a, b, c, d, Arefi and Zenkour 2017 a, b, c, d)

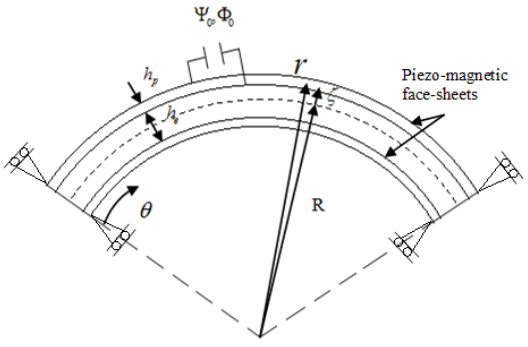

Fig. 1 The schematic diagram of a sandwich curved beam

$$E_r = -\frac{\partial \breve{\psi}}{\partial r}, \quad E_\theta = -\frac{1}{r}\frac{\partial \breve{\psi}}{\partial \theta},$$
$$H_r = -\frac{\partial \breve{\phi}}{\partial r}, \quad H_\theta = -\frac{1}{r}\frac{\partial \breve{\phi}}{\partial \theta}. \tag{5}$$

The curved beam is subjected to applied electric and magnetic potentials. To apply initial electric and magnetic potential at top and bottom of face-sheets, a linear function of radial components is used. In addition for general distribution of electric and magnetic potentials, a cosine function is used to apply homogenized electric and magnetic boundary conditions. The electric and magnetic fields are assumed as combination of a cosine function along the thickness direction and an unknown function along the circumferential direction θ (Arefi and Zenkour 2016 a, b, c, d, 2017 a, b, c, d)

$$\breve{\psi}(r,\theta) = -\psi(\theta)\cos\left(\frac{\pi}{h_p}\rho\right) + \frac{2\psi_0}{h_p}\rho,$$
$$\breve{\phi}(r,\theta) = -\phi(\theta)\cos\left(\frac{\pi}{h_p}\rho\right) + \frac{2\phi_0}{h_p}\rho, \tag{6}$$

in which ψ_0, ϕ_0 are applied electric and magnetic potentials, $\rho = \zeta \pm \frac{h_e}{2} \pm \frac{h_p}{2}$ for top and bottom piezo-magnetic face-sheets. Substitution of electric and magnetic potential into Eq. (6) gives electric and magnetic fields as follows

$$E_r = -\frac{\pi}{h_p}\psi\sin\left(\frac{\pi}{h_p}\rho\right) - \frac{2\psi_0}{h_p}, \quad E_\theta = \frac{1}{r}\frac{\partial\psi}{\partial\theta}\cos\left(\frac{\pi}{h_p}\rho\right),$$
$$H_r = -\frac{\pi}{h_p}\phi\sin\left(\frac{\pi}{h_p}\rho\right) - \frac{2\phi_0}{h_p}, \quad H_\theta = \frac{1}{r}\frac{\partial\phi}{\partial\theta}\cos\left(\frac{\pi}{h_p}\rho\right). \tag{7}$$

The electric displacement and magnetic induction along the radial and circumferential directions are derived as (Arefi and Zenkour 2016 a, b, c, d)

$$D_r^p = e_{r\theta\theta}^p \varepsilon_\theta + \epsilon_{rr}^p E_r + m_{rr}^p H_r,$$
$$D_\theta^p = e_{\theta r\theta}^p \gamma_{r\theta} + \epsilon_{\theta\theta}^p E_\theta + m_{\theta\theta}^p H_\theta, \tag{8}$$

$$B_r^p = q_{r\theta\theta}^p \varepsilon_\theta + m_{rr}^p E_r + \mu_{rr}^p H_r,$$
$$B_\theta^p = q_{\theta r\theta}^p \gamma_{r\theta} + m_{\theta\theta}^p E_\theta + \mu_{\theta\theta}^p H_\theta, \tag{9}$$

in which m_{ij}^p and μ_{ij}^p are dielectric and electromagnetic coefficients. In this stage and using the Hamilton's principle $\int \delta(T - U + V)\mathrm{d}t = 0$, we can derive the governing equations of motion. The variation of strain energy δU is defined as (Zenkour and Arefi 2017 a, b)

$$\delta U = \iiint_v (\sigma_{\theta\theta}\delta\varepsilon_{\theta\theta} + \sigma_{r\theta}\delta\varepsilon_{r\theta} - D_r\delta E_r - D_\theta\delta E_\theta - B_r\delta H_r - B_\theta\delta H_\theta)\mathrm{d}V. \tag{10}$$

By substitution of volume element $\mathrm{d}V = br\mathrm{d}r\mathrm{d}\theta = b(R+\zeta)\mathrm{d}\zeta\mathrm{d}\theta$ and variation of strains, electric and magnetic fields into Eq. (10), we will have

$$\delta U = \iiint_v \Big\{\sigma_{\theta\theta}\Big[\frac{\delta u_r}{R+\zeta} + \frac{1}{R+\zeta}\frac{\mathrm{d}\delta u_\theta}{\mathrm{d}\theta} + \frac{\chi}{R+\zeta}\frac{\mathrm{d}\delta u_1}{\mathrm{d}\theta}\Big] + \sigma_{r\theta}\Big[\frac{1}{R+\zeta}\frac{\mathrm{d}\delta u_r}{\mathrm{d}\theta} - \frac{\delta u_\theta}{R+\zeta} + \frac{R}{R+\zeta}\delta\chi\Big] - D_r\frac{\pi}{h_p}\delta\psi\sin\left(\frac{\pi}{h_p}\rho\right) - D_\theta\frac{1}{r}\frac{\partial\delta\psi}{\partial\theta}\cos\left(\frac{\pi}{h_p}\rho\right) + B_r\frac{\pi}{h_p}\delta\phi\sin\left(\frac{\pi}{h_p}\rho\right) - B_\theta\frac{1}{r}\frac{\partial\delta\phi}{\partial\theta}\cos\left(\frac{\pi}{h_p}\rho\right)\Big\}(R+\zeta)\mathrm{d}\zeta\mathrm{d}\theta. \tag{11}$$

By definition of resultant of mechanical, electrical and magnetic components, we will have variation of strain energy as follows

$$\delta U = \iiint_v \Big[N_{\theta\theta}\delta u_r + N_{\theta\theta}\frac{\mathrm{d}\delta u_\theta}{\mathrm{d}\theta} + M_{\theta\theta}\frac{\mathrm{d}\delta\chi}{\mathrm{d}\theta} + N_{r\theta}\frac{\mathrm{d}\delta u_r}{\mathrm{d}\theta} + (RN_{r\theta} + M_{r\theta})\delta\chi - N_{r\theta}\delta u_\theta - M_{r\theta}\delta\chi + \bar{D}_r\delta\psi - \bar{D}_\theta\frac{\partial\delta\psi}{\partial\theta} + \bar{B}_r\delta\phi - \bar{B}_\theta\frac{\partial\delta\phi}{\partial\theta}\Big]\mathrm{d}\theta, \tag{12}$$

in which the resultant components are defined as (Arefi and Zenkour 2016 a, b, c, d)

$$\{N_{\theta\theta}, N_{r\theta}\} = \int_{-\frac{h_e}{2}-h_p}^{-\frac{h_e}{2}}\{\sigma_{\theta\theta}^p, \sigma_{r\theta}^p\}\mathrm{d}\zeta + \int_{-\frac{h_e}{2}}^{+\frac{h_e}{2}}\{\sigma_{\theta\theta}^c, \sigma_{r\theta}^c\}\mathrm{d}\zeta + \int_{\frac{h_e}{2}}^{\frac{h_e}{2}+h_p}\{\sigma_{\theta\theta}^p, \sigma_{r\theta}^p\}\mathrm{d}\zeta$$
$$\{M_{\theta\theta}, M_{r\theta}\} = \int_{-\frac{h_e}{2}-h_p}^{-\frac{h_e}{2}}\zeta\{\sigma_{\theta\theta}^p, \sigma_{r\theta}^p\}\mathrm{d}\zeta + \int_{-\frac{h_e}{2}}^{+\frac{h_e}{2}}\zeta\{\sigma_{\theta\theta}^c, \sigma_{r\theta}^c\}\mathrm{d}\zeta + \int_{\frac{h_e}{2}}^{\frac{h_e}{2}+h_p}\zeta\{\sigma_{\theta\theta}^p, \sigma_{r\theta}^p\}\mathrm{d}\zeta,$$
$$\{\bar{D}_r, \bar{B}_r\} = \int_{-\frac{h_e}{2}-h_p}^{-\frac{h_e}{2}}(R+\zeta)\frac{\pi}{h_p}\sin\left(\frac{\pi}{h_p}\rho\right)\{D_r, B_r\}\mathrm{d}\zeta + \int_{\frac{h_e}{2}}^{\frac{h_e}{2}+h_p}(R+\zeta)\frac{\pi}{h_p}\sin\left(\frac{\pi}{h_p}\rho\right)\{D_r, B_r\}\mathrm{d}\zeta$$
$$\{\bar{D}_\theta, \bar{B}_\theta\} = \int_{-\frac{h_e}{2}-h_p}^{-\frac{h_e}{2}}\cos\left(\frac{\pi}{h_p}\rho\right)\{D_\theta, B_\theta\}\mathrm{d}\zeta + \int_{\frac{h_e}{2}}^{\frac{h_e}{2}+h_p}\cos\left(\frac{\pi}{h_p}\rho\right)\{D_\theta, B_\theta\}\mathrm{d}\zeta \tag{13}$$

Applying the integration by part on Eq. (12) yields

$$\delta U = \iiint_v \Big[N_{\theta\theta}\delta u_r - \frac{\mathrm{d}N_{\theta\theta}}{\mathrm{d}\theta}\delta u_\theta - \frac{\mathrm{d}M_{\theta\theta}}{\mathrm{d}\theta}\delta\chi - \frac{\mathrm{d}N_{r\theta}}{\mathrm{d}\theta}\delta u_r + (RN_{r\theta} + M_{r\theta})\delta\chi - N_{r\theta}\delta u_\theta - M_{r\theta}\delta\chi + \bar{D}_r\delta\psi - \bar{D}_\theta\frac{\partial\delta\psi}{\partial\theta} + \bar{B}_r\delta\phi - \bar{B}_\theta\frac{\partial\delta\phi}{\partial\theta}\Big]\mathrm{d}\theta \tag{14}$$

In addition, the variation of energy due to external works is given by

$$\delta V = \iint_A (R_f - q)\delta u_r \mathrm{d}A, \tag{15}$$

in which R_f is reaction of Pasternak's foundation. This reaction is defined by

$$R_f = K_1 u_r - K_2\nabla^2 u_r, \tag{16}$$

where ∇^2 is Laplace operator in polar coordinate system, K_1 and K_2 are spring and shear parameters of foundation. By substitution of $\nabla^2 = \frac{1}{r^2}\frac{\partial^2}{\partial\theta^2}$ into above equation, we will have the reaction of foundation as follows

$$R_f = K_1 u_r - K_2 \frac{1}{r^2}\frac{\partial^2 u_r}{\partial \theta^2}. \tag{17}$$

Variation of kinetic energy is defined as

$$\delta T = \iint_A \rho[\dot{u}_r \delta \dot{u}_r + (\dot{u}_\theta + \zeta\dot{\chi})(\delta\dot{u}_\theta + \zeta\delta\dot{\chi})]b(R+\zeta)\mathrm{d}\zeta\mathrm{d}\theta. \tag{18}$$

Integration by part yields

$$\delta T = -\iint_A (A_1\ddot{u}_r\delta u_r + A_1\ddot{u}_\theta\delta u_\theta + A_2\ddot{\chi}\delta u_\theta + A_2\ddot{u}_\theta\delta\chi + A_3\ddot{\chi}\delta\chi)\mathrm{d}\theta, \tag{19}$$

in which the integration constants A_1, A_2 and A_3 are expressed in Appendix. Substitution of variations of strain energy, kinetic energy and energy due to external works into Hamilton's principle leads to the following five governing equations of motion

$$\begin{gathered}
\delta u_r\colon\ -N_{\theta\theta} + \frac{\mathrm{d}N_{r\theta}}{\mathrm{d}\theta} + \left(K_1 u_r - K_2 \frac{1}{\left(R - \frac{h_e}{2} - h_p\right)^2}\frac{\mathrm{d}^2 u_r}{\mathrm{d}\theta^2} - q\right) = A_1\ddot{u}_r,\\
\delta u_\theta\colon\ \frac{\mathrm{d}N_{\theta\theta}}{\mathrm{d}\theta} + N_{r\theta} = A_1\ddot{u}_\theta + A_2\ddot{\chi},\\
\delta\chi\colon\ \frac{\mathrm{d}M_{\theta\theta}}{\mathrm{d}\theta} - RN_{r\theta} = A_2\ddot{u}_\theta + A_3\ddot{\chi},\\
\delta\psi\colon\ \bar{D}_r + \frac{\mathrm{d}\bar{D}_\theta}{\mathrm{d}\theta} = 0,\\
\delta\phi\colon\ \bar{B}_r + \frac{\mathrm{d}\bar{B}_\theta}{\mathrm{d}\theta} = 0.
\end{gathered} \tag{20}$$

In this stage, we can calculate the resultant components in terms of displacement and rotation components and electric and magnetic potentials. These resultants are defined as

$$\begin{gathered}
N_{\theta\theta} = A_4\left(u_r + \frac{\mathrm{d}u_\theta}{\mathrm{d}\theta}\right) + A_5\frac{\mathrm{d}\chi}{\mathrm{d}\theta} + A_6\psi + A_7\phi + N_\psi + N_\phi,\\
M_{\theta\theta} = A_5\left(u_r + \frac{\mathrm{d}u_\theta}{\mathrm{d}\theta}\right) + A_8\frac{\mathrm{d}\chi}{\mathrm{d}\theta} + A_9\psi + A_{10}\phi + M_\psi + M_\phi,\\
N_{r\theta} = A_{11}\left(\frac{\mathrm{d}u_r}{\mathrm{d}\theta} - u_\theta\right) + (A_{12} - A_{13})\chi - A_{14}\frac{\partial\psi}{\partial\theta} - A_{15}\frac{\partial\phi}{\partial\theta},\\
\bar{D}_r = A_{16}\left(u_r + \frac{\mathrm{d}u_\theta}{\mathrm{d}\theta}\right) + A_{17}\frac{\mathrm{d}\chi}{\mathrm{d}\theta} - A_{18}\psi - A_{19}\phi - D_\psi - D_\phi,\\
\bar{B}_r = A_{20}\left(u_r + \frac{\mathrm{d}u_\theta}{\mathrm{d}\theta}\right) + A_{21}\frac{\mathrm{d}\chi}{\mathrm{d}\theta} - A_{19}\psi - A_{22}\phi - B_\psi - B_\phi,\\
\bar{D}_\theta = A_{23}\left(\frac{\mathrm{d}u_r}{\mathrm{d}\theta} - u_\theta\right) + (A_{24} - A_{25})\chi + A_{29}\frac{\partial\psi}{\partial\theta} + A_{30}\frac{\partial\phi}{\partial\theta}\\
\bar{B}_\theta = A_{26}\left(\frac{\mathrm{d}u_r}{\mathrm{d}\theta} - u_\theta\right) + (A_{27} - A_{28})\chi + A_{30}\frac{\partial\psi}{\partial\theta} + A_{31}\frac{\partial\phi}{\partial\theta}
\end{gathered} \tag{21}$$

in which the integration constants are expressed in Appendix. Substitution of above resultant components into five governing equations of motion leads to

$$\begin{gathered}
\delta u_r\colon\ A_{11}\frac{\mathrm{d}^2 u_r}{\mathrm{d}\theta^2} - A_4 u_r - (A_4 + A_{11})\frac{\mathrm{d}u_\theta}{\mathrm{d}\theta} + (A_{12} - A_{13} - A_5)\frac{\mathrm{d}\chi}{\mathrm{d}\theta} - A_{14}\frac{\mathrm{d}^2\psi}{\mathrm{d}\theta^2} - A_{15}\frac{\mathrm{d}^2\phi}{\mathrm{d}\theta^2}\\
-A_6\psi - A_7\phi + K_1 u_r - K_2\frac{1}{r^2}\frac{\mathrm{d}^2 u_r}{\mathrm{d}\theta^2} - q = A_1\ddot{u}_r + N_\psi + N_\phi,\\
\delta u_\theta\colon\ (A_4 + A_{11})\frac{\mathrm{d}u_r}{\mathrm{d}\theta} + A_4\frac{\mathrm{d}^2 u_\theta}{\mathrm{d}\theta^2} - A_{11}u_\theta + A_5\frac{\mathrm{d}^2\chi}{\mathrm{d}\theta^2} + (A_{12} - A_{13})\chi + (A_6 - A_{14})\frac{\mathrm{d}\psi}{\mathrm{d}\theta}\\
+(A_7 - A_{15})\frac{\mathrm{d}\phi}{\mathrm{d}\theta} = A_1\ddot{u}_\theta + A_2\ddot{\chi} - \frac{\mathrm{d}N_\psi}{\mathrm{d}\theta} - \frac{\mathrm{d}N_\phi}{\mathrm{d}\theta},\\
\delta\chi\colon\ (A_5 - RA_{11})\frac{\mathrm{d}u_r}{\mathrm{d}\theta} + A_5\frac{\mathrm{d}^2 u_\theta}{\mathrm{d}\theta^2} + RA_{11}u_\theta + A_8\frac{\mathrm{d}^2\chi}{\mathrm{d}\theta^2} - R(A_{12} - A_{13})\chi + (A_9 + RA_{14})\frac{\mathrm{d}\psi}{\mathrm{d}\theta}\\
+(A_{10} + RA_{15})\frac{\mathrm{d}\phi}{\mathrm{d}\theta} = A_2\ddot{u}_\theta + A_3\ddot{\chi} - \frac{\mathrm{d}M_\psi}{\mathrm{d}\theta} - \frac{\mathrm{d}M_\phi}{\mathrm{d}\theta},\\
\delta\psi\colon\ A_{23}\frac{\mathrm{d}^2 u_r}{\mathrm{d}\theta^2} + A_{16}u_r + (A_{16} - A_{23})\frac{\mathrm{d}u_\theta}{\mathrm{d}\theta} + (A_{17} + A_{24} - A_{25})\frac{\mathrm{d}\chi}{\mathrm{d}\theta} + A_{29}\frac{\mathrm{d}^2\psi}{\mathrm{d}\theta^2}\\
+A_{30}\frac{\mathrm{d}^2\phi}{\mathrm{d}\theta^2} - A_{18}\psi - A_{19}\phi = D_\psi + D_\phi,\\
A_{26}\frac{\mathrm{d}^2 u_r}{\mathrm{d}\theta^2} - A_{20}u_r + (A_{20} - A_{26})\frac{\mathrm{d}u_\theta}{\mathrm{d}\theta} + (A_{21} + A_{27} - A_{28})\frac{\mathrm{d}\chi}{\mathrm{d}\theta} - A_{30}\frac{\mathrm{d}^2\psi}{\mathrm{d}\theta^2} - A_{31}\frac{\mathrm{d}^2\phi}{\mathrm{d}\theta^2}\\
-A_{19}\psi - A_{22}\phi = B_\psi + B_\phi.
\end{gathered} \tag{22}$$

3. Solution procedure

In this section, the solution procedure for free vibration and electro-magneto-mechanical bending results are developed. Before presentation of solution procedure, the required mechanical, electrical and magnetic boundary conditions must be expressed. These boundary conditions are mentioned as

$$\theta = 0, L/R \to u_r = \psi = \phi = 0, \quad N_\theta = M_\theta = 0 \quad \{u_\theta, \chi \neq 0\}. \tag{23}$$

The proposed solutions for a simply-supported curved sandwich beam are expressed as (Arefi and Zenkour 2016 a, b, c, d)

$$\begin{Bmatrix} [u_\theta, \chi] \\ [u_r, \psi, \phi] \end{Bmatrix} = \mathrm{e}^{i\omega t}\sum_{m=1,3,5}\begin{Bmatrix} [U_\theta, X]\cos(\beta_m\theta) \\ [U_r, \Psi, \Phi]\sin(\beta_m\theta) \end{Bmatrix} \tag{24}$$

in which $\beta_m = m\pi R/L$. Substitution of proposed solution into governing equations of motion leads to below equation

$$[K]\{X\} = \{F\} + \omega^2[M]\{X\} \tag{25}$$

in which $\{X\} = \{U_r, U_\theta, \mathrm{X}, \Psi, \Phi\}$ is an unknown vector corresponding to five unknown functions. The symmetric elements of the matrix $[K]$ and $[M]$ are expressed as

$$\begin{gathered}
K_{11} = -A_{11}\beta_m^2 - A_4 + K_1 + K_2\frac{1}{\left(R - \frac{h}{2} - \frac{h_p}{2}\right)^2}\beta_m^2, \quad K_{12} = (A_4 + A_{11})\beta_1,\\
K_{13} = (A_5 - A_{12} + A_{13})\beta_m, \quad K_{14} = A_{14}\beta_m^2 - A_6, \quad K_{15} = A_{15}\beta_m^2 - A_7, \quad M_{11} = A_1,\\
K_{21} = (A_4 + A_{11})\beta_m, \quad K_{22} = -A_4\beta_m^2 - A_{11}, \quad K_{23} = -A_5\beta_m^2 + A_{12} - A_{13}\\
K_{24} = (A_6 - A_{14})\beta_m, \quad K_{25} = (A_7 - A_{15})\beta_m, \quad M_{22} = A_1, \quad M_{23} = A_2\\
K_{31} = (A_5 - RA_{11})\beta_m, \quad K_{32} = -A_5\beta_m^2 + RA_{11}, \quad K_{33} = -A_8\beta_m^2 - R(A_{12} - A_{13})\chi,\\
K_{34} = (A_9 + RA_{14})\beta_m, \quad K_{35} = (A_{10} + RA_{15})\beta_m, \quad M_{32} = A_2, \quad M_{33} = A_3\\
K_{41} = A_{23}\beta_m^2 - A_{16}, \quad K_{42} = (A_{16} - A_{23})\beta_m, \quad K_{43} = (A_{17} + A_{24} - A_{25})\beta_m\\
K_{44} = A_{29}\beta_m^2 + A_{18}, \quad K_{45} = A_{30}\beta_m^2 + A_{19}\\
K_{51} = A_{26}\beta_m^2 - A_{20}u_r, \quad K_{52} = (A_{20} - A_{26})\beta_1, \quad K_{53} = (A_{21} + A_{27} - A_{28})\beta_m\\
K_{54} = A_{30}\beta_m^2 + A_{19}, \quad K_{55} = A_{31}\beta_m^2 + A_{22}
\end{gathered} \tag{26}$$

In addition, the elements of the force vector $\{F\}$ are expressed as

$$F_1 = N_\psi + N_\phi - R_f + q, \quad F_2 = -\frac{\mathrm{d}N_\psi}{\mathrm{d}\theta} - \frac{\mathrm{d}N_\phi}{\mathrm{d}\theta}, \quad F_3 = -\frac{\mathrm{d}M_\psi}{\mathrm{d}\theta} - \frac{\mathrm{d}M_\phi}{\mathrm{d}\theta}, \quad F_4 = -D_\psi - D_\phi, \quad F_5 = -B_\psi - B_\phi. \tag{27}$$

4. Results and discussions

In this section, the numerical results of the problem are presented. Before presentation of numerical results, the material properties of elastic core and piezomagnetic layers must be introduced (Hou and Leung 2004)

Core

$$E = 210 \text{ GPa}, \quad v = 0.3.$$

Piezomagnetic face-sheets (Arefi and Zenkour 2017 a, b)

$$C^p_{\theta\theta\theta\theta} = 286 \text{ GPa}, \quad C^p_{r\theta r\theta} = 45.3 \text{ GPa},$$

$$e^p_{\theta\theta r} = e^p_{r\theta\theta} = -4.4 \text{ (C/m}^2\text{)}, \quad e^p_{\theta r\theta} = 11.6 \text{ (C/m}^2\text{)},$$

$$q^p_{\theta\theta r} = q^p_{r\theta\theta} = 580.3 \text{ (N/Am)}, \quad q^p_{\theta r\theta} = 550 \text{ (N/Am)},$$

$$\epsilon^p_{rr} = 9.3 \times 10^{-11} \text{ (C/mV)}, \quad \epsilon^p_{\theta\theta} = 8 \times 10^{-11} \text{ (C/mV)},$$

$$m^p_{rr} = 3 \times 10^{-12} \text{ (Ns/CV)}, \quad m^p_{\theta\theta} = 5 \times 10^{-12} \text{ (Ns/CV)},$$

$$\mu^p_{rr} = 1.57 \times 10^{-4} \text{ (Ns}^2\text{/C}^2\text{)}, \quad \mu^p_{\theta\theta} = -5.9 \times 10^{-4} \text{ (Ns}^2\text{/C}^2\text{)}.$$

Comparison and validation

To validate the present formulation and corresponding analytical and numerical results, comparison between results of our formulation with a valid reference (Shi and Zhong 2008) is performed. For this comparison, radial displacement u_r is selected to plot in terms of applied electric potential Ψ_0 and angle of curved beam θ. Shown in Fig. 2 is influence of applied electric potential on the variation of radial displacement u_r based on present formulation and results of Shi and Zhong (2008).

In addition, comparison between current and previous results (Shi and Zhang 2008) for radial displacement u_r in terms of angle of curved beam θ for $\Psi_0 = 100$ V is presented in Fig. 3. One can conclude that our numerical results in this paper are in good agreement with reference.

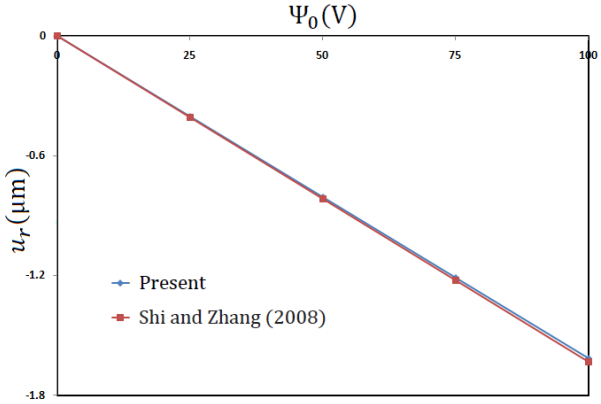

Fig. 2 Variation of radial displacement u_r(μm) in terms of applied electric potential Ψ_0(V)

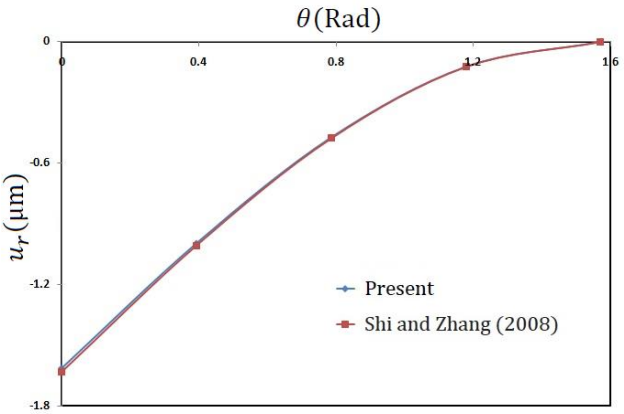

Fig. 3 Variation of radial displacement u_r(μm) in terms of angle of beam θ(Rad)

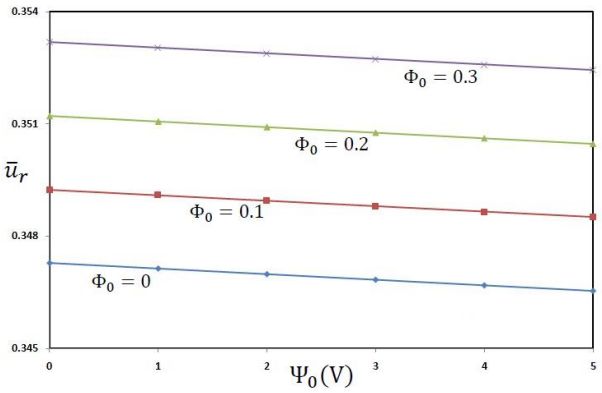

Fig. 4 The non-dimensional value of radial displacement $\bar{u}_r$ in terms of applied electric and magnetic potential Ψ_0 and Φ_0

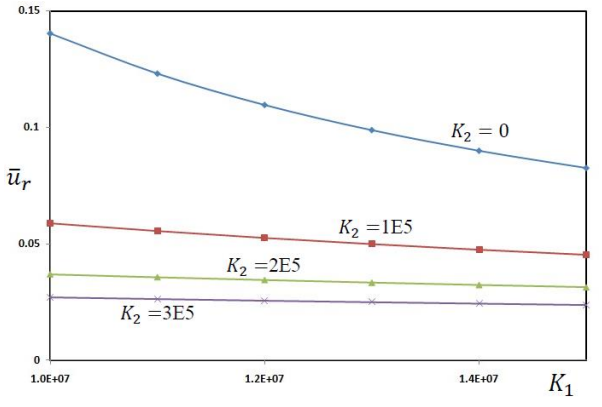

Fig. 5 The non-dimensional value of radial displacement $\bar{u}_r$ in terms of two parameters of Pasternak's foundation K_1 and K_2

Shown in Fig. 4 is the non-dimensional value of radial displacement $\bar{u}_r = U_r/h$ in terms of applied electric and magnetic potential Ψ_0 and Φ_0. The numerical results in this figure indicates that increase of applied electric potential Ψ_0 leads to decrease of radial displacement while increase of applied magnetic potential Φ_0 leads to increase of radial displacement. Figure 5 shows the variation of non-dimensional value of radial displacement $\bar{u}_r$ in terms of two parameters of Pasternak's foundation K_1 and K_2. It is observed that the radial displacement is decreased uniformly with increase of both parameters. This decrease is due to increase of stiffness of foundation.

The influences of applied electric and magnetic potentials Ψ_0 and Φ_0 on the non-dimensional value of circumferential displacement $\bar{u}_\theta$ are depicted in Fig. 6. The same behavior expressed for Fig. 2 can be presented in this figure. Fig. 7 shows the variation of non-dimensional value of $\bar{u}_\theta$ in terms of two parameters of Pasternak's foundation K_1 and K_2.

Fig. 8 shows the variation of rotation of sandwich curved beam in terms of applied electric and magnetic potential Ψ_0 and Φ_0. This figure shows that increase of applied electric potential leads to decrease of rotation, while increase of applied magnetic potential leads to increase of rotation of sandwich curved beam. Figure 9 shows the influence of two parameters of foundation on the rotation of curved beam.

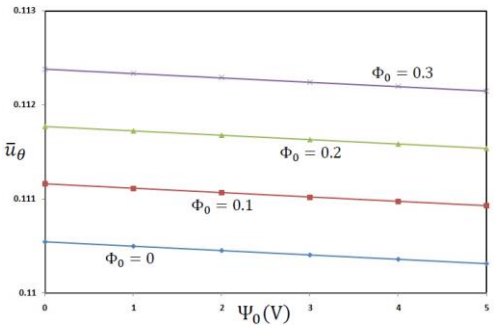

Fig. 6 The non-dimensional value of circumferential displacement $\bar{u}_\theta$ in terms of applied electric and magnetic potential Ψ_0 and Φ_0

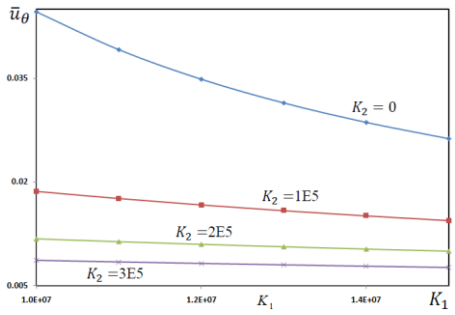

Fig. 7 The non-dimensional value of circumferential displacement $\bar{u}_\theta$ in terms of two parameters of Pasternak's foundation K_1 and K_2

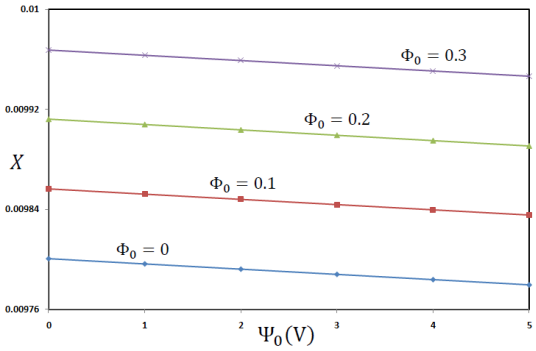

Fig. 8 Maximum beam rotation X in terms of applied electric and magnetic potential Ψ_0 and Φ_0

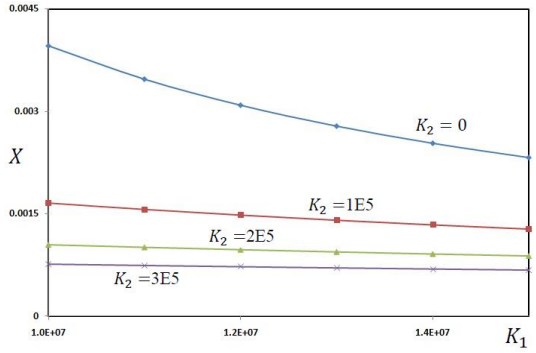

Fig. 9 Maximum beam rotation X in terms of two parameters of Pasternak's foundation K_1 and K_2

The influence of important parameters of the problem can be studied on the magneto-electric results of the sandwich curved beam in Figs. 10-13. Fig. 10 present interesting results on the effect of electro-magnetic coupling loads. One can conclude that increase of applied electric potential leads to decrease of maximum electric potential through thickness direction. Furthermore, it can be discussed that increase of applied magnetic potential significantly increases maximum electric potential. Fig. 11 shows that increase of two parameters of foundation decreases maximum electric potential.

The maximum value of magnetic potential through thickness direction in terms of applied electric and magnetic potentials is presented in Fig. 12. It can be concluded that decrease of applied electric potential and increase of applied magnetic potential increases maximum magnetic potential of curved piezo-magnetic face-sheets. Fig. 13 shows the variation of maximum magnetic potential in terms of two parameters of foundation.

The non-dimensional fundamental natural frequencies $\bar{\omega} = \omega L^2\sqrt{\rho/EI}$ of sandwich curved beam in terms of two non-dimensional parameters of foundation $\bar{K}_1 = K_1 L^3/EI$ and $\bar{K}_2 = K_2 L/EI$ are presented in Fig. 14. It is observed that the natural frequencies are increased with increase of two parameters of foundation. This increase is due to increase of stiffness of foundation.

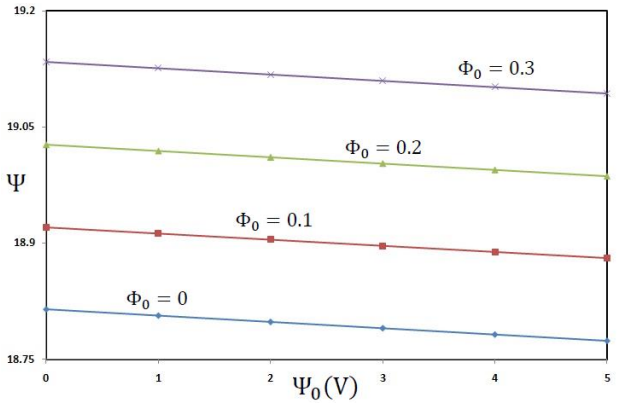

Fig. 10 The maximum value of electric potential Ψ through thickness direction in terms of applied electric and magnetic potential Ψ_0 and Φ_0

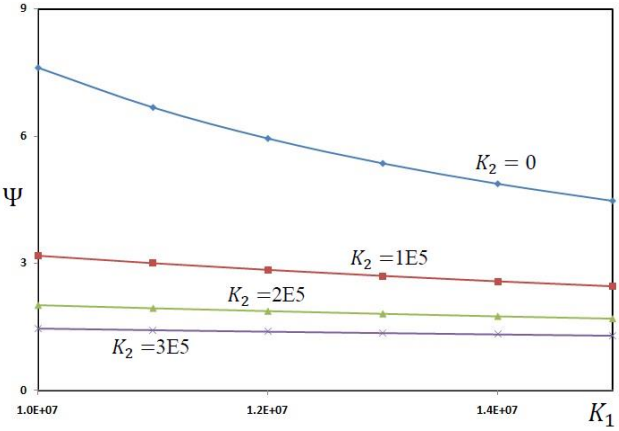

Fig. 11 The maximum value of electric potential Ψ through thickness direction in terms of two parameters of Pasternak's foundation K_1 and K_2

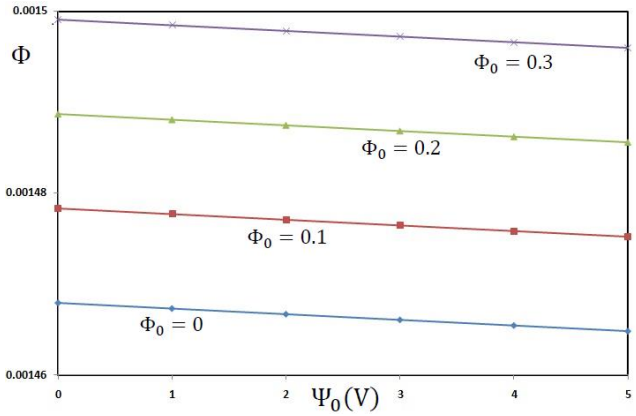

Fig. 12 The maximum value of magnetic potential Φ through thickness direction in terms of applied electric and magnetic potential Ψ_0 and Φ_0

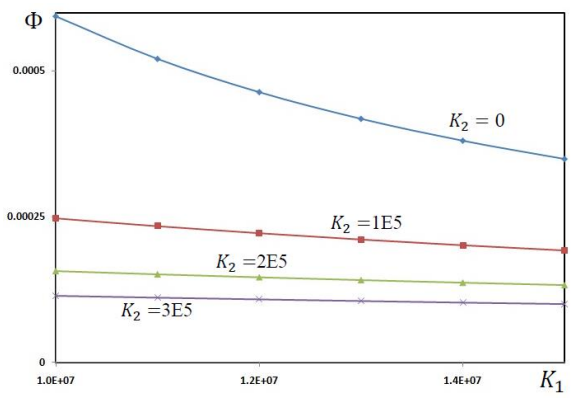

Fig. 13 The maximum value of magnetic potential Φ through thickness direction in terms of two parameters of Pasternak's foundation K_1 and K_2

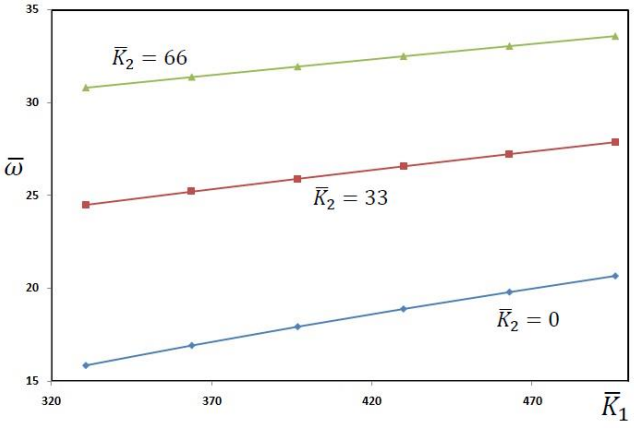

Fig. 14 The fundamental natural frequencies $\bar{\omega}$ of sandwich curved beam in terms of two parameters of Pasternak's foundation $\bar{K}_1$ and $\bar{K}_2$

5. Conclusions

Electro-magneto-elastic bending and free vibration analysis of a sandwich curved beam including an elastic core and two curved piezo-magnetic face-sheets was presented in this paper. The model was subjected to applied electric and magnetic potentials resting on Pasternak's foundation. Hamilton's principle was employed to derive five governing equations of motion in terms of two displacement components, one rotation component and two electric and magnetic potentials. The influences of important parameters of loading and electro-magnetic loadings were studied and discussed on the bending and vibration results of the problem as:

- The influence of spring and shear parameters of foundation was discussed on the fundamental frequencies of curved beam. The numerical results indicate that fundamental frequencies are increased

with increase of both parameters of foundation due to increase of foundation stiffness.

- Piezomagnetic face-sheets can be subjected to applied electric and magnetic potentials. These parameters of loading can control the displacements or stresses in curved beam. The numerical results indicate that increase of applied electric potential decrease all mechanical, electrical and magnetic components. Furthermore, it can be concluded that increase of magnetic potential increases electro-magneto-mechanical components.
- Pasternak's foundation with two parameters can strongly change the behavior of curved sandwich beam. The results indicate that increase of spring and shear parameters of foundation decreases radial and circumferential displacements, rotation and electric and magnetic potentials.

References

Arefi, M. (2014), "A complete set of equations for piezo-magnetoelastic analysis of a functionally graded thick shell of revolution", *Lat. Amer. J. Solids. Struct.*, **11**(11), 2073-2092.

Arefi, M. and Khoshgoftar, M.J. (2014), "Comprehensive piezo-thermo-elastic analysis of a thick hollow spherical shell", *Smart. Struct. Syst.*, **14**(2), 225-246.

Arefi, M. (2015), "Elastic solution of a curved beam made of functionally graded materials with different cross sections", *Steel. Compos. Struct.*, **18**(3), 659-672.

Arefi, M. and Zenkour, A.M. (2016a), "Free vibration, wave propagation and tension analyses of a sandwich micro/nano rod subjected to electric potential using strain gradient theory", *Mater. Res. Express.*, **3**(11), 115704.

Arefi, M. and Zenkour A.M. (2016b), "Employing sinusoidal shear deformation plate theory for transient analysis of three layers sandwich nanoplate integrated with piezo-magnetic face-sheets", *Smart. Mater. Struct.*, **25**(11), 115040.

Arefi, M. and Zenkour A.M. (2016c), "A simplified shear and normal deformations nonlocal theory for bending of functionally graded piezomagnetic sandwich nanobeams in magneto-thermo-electric environment", *J. Sandw. Struct. Mater.*, **18**(5), 624-651.

Arefi, M. and Zenkour A.M. (2016d), "Nonlocal electro-thermo-mechanical analysis of a sandwich nanoplate containing a Kelvin–Voigt viscoelastic nanoplate and two piezoelectric layers", *Acta Mech.*, **228**(2), 475-493.

Arefi, M. and Rahimi, G.H. (2014), "Application of shear deformation theory for two dimensional electro-elastic analysis of a FGP cylinder", *Smart. Struct. Syst.*, **13**(1), 1-24.

Arefi, M. and Zenkour, A.M. (2017a), "Thermo-electro-mechanical bending behavior of sandwich nanoplate integrated with piezoelectric face-sheets based on trigonometric plate theory", *Compos. Struct.*,**162**, 108-122.

Arefi, M. and Zenkour, A.M. (2017b), "Vibration and bending analysis of a sandwich microbeam with two integrated piezo-magnetic face-sheets", *Compos. Struct.* **159**, 479-490.

Arefi, M. and Zenkour, A.M. (2017c), "Size-dependent vibration and bending analyses of the piezomagnetic three-layer nanobeams", *Appl. Phys. A.*, **123**(3), 202.

Arefi, M. and Zenkour, A.M. (2017d), "Transient analysis of a three-layer microbeam subjected to electric potential", *Int. J. Smart. Nano. Mater.*, **8**(1), 20-40.

Arefi, M. and Zenkour, A.M. (2017e), "Wave propagation analysis of a functionally graded magneto-electro-elastic nanobeam rest on Visco-Pasternak foundation", *Mech. Res. Commun.*, **79**, 51-62.

Arslan, E. and Usta, R. (2014), "Mechanical and electrical fields of piezoelectric curved sensors", *Arch. Mech.*, **66**(5), 329-342.

Hosseini, S.A.H. and Rahmani, O. (2016a), "Free vibration of shallow and deep curved FG nanobeam via nonlocal Timoshenko curved beam model", *Appl. Phys. A*, **122**,169.

Hosseini, S.A.H. and Rahmani, O. (2016b), "Thermomechanical vibration of curved functionally graded nanobeam based on nonlocal elasticity", *J. Therm. Stresses*, **39**(10), 1252-1267.

Hou, P.F. and Leung, A.Y.T. (2004), "The transient responses of magneto-electro-elastic hollow cylinders", *Smart. Mater. Struct.*, **13**, 762-776.

Kananipour, H., Ahmadi, M. and Chavoshi, H., (2014), "Application of nonlocal elasticity and DQM to dynamic analysis of curved nanobeams", *Lat. Amer. J. Solids. Struct.*, **11**(5), 848-853.

Koutsawa, Y. and Daya, E.M. (2007), "Static and free vibration analysis of laminated glass beam on viscoelastic supports", *Int. J. Solids. Struct.*, **44**, 8735-8750.

Kuang, Y.D., Li, G.Q., Chen, C.Y. and Min, Q. (2007), "The static responses and displacement control of circular curved beams with piezoelectric actuators", *Smart. Mater. Struct.*, **16**, 1016-1024.

Shi, Z.F. (2005), "Bending behavior of piezoelectric curved actuator", *Smart. Mater. Struct.*, **14**, 835-842.

Shi, Z.F. and Zhang, T. (2008), "Bending analysis of a piezoelectric curved actuator with a generally graded property for the piezoelectric parameter", *Smart. Mater. Struct.*, **17**(4): 045018 (7pp).

Sun, D.C. and Tong, L. (2001), "Sensor/actuator equations for curved piezoelectric fibers and vibration control of composite beams using fiber modal actuators/sensors", *J. Sound. Vib.*, **241**(2), 297-314.

Sun, D. and Tong, L. (2002), "Modeling and analysis of curved beams with debonded piezoelectric sensor/actuator patches", *Int. J. Mech. Sci.*, **44**, 1755-1777.

Susanto, K. (2009), "Vibration analysis of piezoelectric laminated slightly curved beams using distributed transfer function method", *Int. J. Solids. Struct.*, **46**, 1564-1573.

Yan, Z. and Jiang, L. (2011), "Electromechanical response of a curved piezoelectric nanobeam with the consideration of surface effects", *J. Phys. D: Appl. Phys.*, **44**, 365301 (8pp).

Zenkour, A.M. and Arefi, M. (2017a), "Nonlocal transient electrothermomechanical vibration and bending analysis of a functionally graded piezoelectric single-layered nanosheet rest on visco-Pasternak foundation", *J. Therm. Stresses.*, **40**(2), 167-184.

Zhou, Y., Nyberg, T.R., Xiong, G., Zhou, H. and Li, S. (2017), "Precise deflection analysis of laminated piezoelectric curved beam", *J. Intel. Mat. Syst. Str.*, In Press.

Zhou, Y., Dong, Y. and Li, S. (2010), "Analysis of a curved beam MEMS piezoelectric vibration energy harvester", *Adv. Mater. Res.*, **139-141**, 1578-1581.

CC

Appendix

$$\{A_1, A_2, A_3\} = \int_{-\frac{h_e}{2}-h_p}^{-\frac{h_e}{2}} \rho^p(R+\zeta)\{1,\zeta,\zeta^2\}\mathrm{d}\zeta + \int_{-\frac{h_e}{2}}^{+\frac{h_e}{2}} \rho(R+\zeta)\{1,\zeta,\zeta^2\}\mathrm{d}\zeta + \int_{\frac{h_e}{2}}^{\frac{h_e}{2}+h_p} \rho(R+\zeta)\{1,\zeta,\zeta^2\}\mathrm{d}\zeta.$$

$$\{\mathrm{A_4}, \mathrm{A_5}, \mathrm{A_8}\} = \int_{-\frac{\mathrm{h_e}}{2}-\mathrm{h_p}}^{-\frac{\mathrm{h_e}}{2}} \frac{\mathrm{C^p_{\theta\theta\theta\theta}}}{\mathrm{R}+\zeta}\{1,\zeta,\zeta^2\}\mathrm{d}\zeta + \int_{-\frac{\mathrm{h_e}}{2}}^{+\frac{\mathrm{h_e}}{2}} \frac{\mathrm{C^c_{\theta\theta\theta\theta}}}{\mathrm{R}+\zeta}\{1,\zeta,\zeta^2\}\mathrm{d}\zeta + \int_{\frac{\mathrm{h_e}}{2}}^{\frac{\mathrm{h_e}}{2}+\mathrm{h_p}} \frac{\mathrm{C^p_{\theta\theta\theta\theta}}}{\mathrm{R}+\zeta}\{1,\zeta,\zeta^2\}\mathrm{d}\zeta,$$

$$\{A_6, A_7, A_9, A_{10}\} = \int_{-\frac{h_e}{2}-h_p}^{-\frac{h_e}{2}} \frac{\pi}{h_p}\sin\left(\frac{\pi}{h_p}\rho\right)\{e^p_{\theta\theta r}, q^p_{\theta\theta r}, \zeta e^p_{\theta\theta r}, \zeta q^p_{\theta\theta r}\}\mathrm{d}\zeta + \int_{\frac{h_e}{2}}^{\frac{h_e}{2}+h_p} \frac{\pi}{h_p}\sin\left(\frac{\pi}{h_p}\rho\right)\{e^p_{\theta\theta r}, q^p_{\theta\theta r}, \zeta e^p_{\theta\theta r}, \zeta q^p_{\theta\theta r}\}\mathrm{d}\zeta,$$

$$\{A_{11}, A_{12}, A_{13}\} = \int_{-\frac{h_e}{2}-h_p}^{-\frac{h_e}{2}} \frac{C^p_{r\theta r\theta}}{R+\zeta}\{1, R+\zeta, \zeta\}\mathrm{d}\zeta + \int_{-\frac{h_e}{2}}^{+\frac{h_e}{2}} \frac{C^c_{r\theta r\theta}}{R+\zeta}\{1, R+\zeta, \zeta\}\mathrm{d}\zeta + \int_{\frac{h_e}{2}}^{\frac{h_e}{2}+h_p} \frac{C^p_{r\theta r\theta}}{R+\zeta}\{1, R+\zeta, \zeta\}\mathrm{d}\zeta,$$

$$\{A_{14}, A_{15}\} = \int_{-\frac{h_e}{2}-h_p}^{-\frac{h_e}{2}} \frac{\cos\left(\frac{\pi}{h_p}\rho\right)}{R+\zeta}\{e^p_{r\theta\theta}, q^p_{r\theta\theta}\}\mathrm{d}\zeta + \int_{\frac{h_e}{2}}^{\frac{h_e}{2}+h_p} \frac{\cos\left(\frac{\pi}{h_p}\rho\right)}{R+\zeta}\{e^p_{r\theta\theta}, q^p_{r\theta\theta}\}\mathrm{d}\zeta,$$

$$\{A_{16}, A_{17}, A_{20}, A_{21}\} = \int_{-\frac{h_e}{2}-h_p}^{-\frac{h_e}{2}} \frac{\pi}{h_p}\sin\left(\frac{\pi}{h_p}\rho\right)\{e^p_{r\theta\theta}, \zeta e^p_{r\theta\theta}, q^p_{r\theta\theta}, \zeta q^p_{r\theta\theta}\}\mathrm{d}\zeta + \int_{\frac{h_e}{2}}^{\frac{h_e}{2}+h_p} \frac{\pi}{h_p}\sin\left(\frac{\pi}{h_p}\rho\right)\{e^p_{r\theta\theta}, \zeta e^p_{r\theta\theta}, q^p_{r\theta\theta}, \zeta q^p_{r\theta\theta}\}\mathrm{d}\zeta,$$

$$\{A_{18}, A_{19}, A_{22}\} = \int_{-\frac{h_e}{2}-h_p}^{-\frac{h_e}{2}} \left[\frac{\pi}{h_p}\sin\left(\frac{\pi}{h_p}\rho\right)\right]^2 (R+\zeta)\{\epsilon^p_{rr}, m^p_{rr}, \mu^p_{rr}\}\mathrm{d}\zeta + \int_{\frac{h_e}{2}}^{\frac{h_e}{2}+h_p} \left[\frac{\pi}{h_p}\sin\left(\frac{\pi}{h_p}\rho\right)\right]^2 (R+\zeta)\{\epsilon^p_{rr}, m^p_{rr}, \mu^p_{rr}\}\mathrm{d}\zeta,$$

$$\{\mathrm{A_{23}}, \mathrm{A_{24}}, \mathrm{A_{25}}, \mathrm{A_{26}}, \mathrm{A_{27}}, \mathrm{A_{28}}\} = \int_{-\frac{h_e}{2}-h_p}^{-\frac{h_e}{2}} \frac{\cos\left(\frac{\pi}{h_p}\rho\right)}{R+\zeta}\{e^p_{\theta r\theta}, (R+\zeta)e^p_{\theta r\theta}, \zeta e^p_{\theta r\theta}, q^p_{\theta r\theta}, (R+\zeta)q^p_{\theta r\theta}, \zeta q^p_{\theta r\theta}\}\mathrm{d}\zeta + \int_{\frac{h_e}{2}}^{\frac{h_e}{2}+h_p} \frac{\cos\left(\frac{\pi}{h_p}\rho\right)}{R+\zeta}\{e^p_{\theta r\theta}, (R+\zeta)e^p_{\theta r\theta}, \zeta e^p_{\theta r\theta}, q^p_{\theta r\theta}, (R+\zeta)q^p_{\theta r\theta}, \zeta q^p_{\theta r\theta}\}\mathrm{d}\zeta,$$

$$\{\mathrm{A_{29}}, \mathrm{A_{30}}, \mathrm{A_{31}}\} = \int_{-\frac{h_e}{2}-h_p}^{-\frac{h_e}{2}} \frac{\cos^2\left(\frac{\pi}{h_p}\rho\right)}{R+\zeta}\{\epsilon^p_{\theta\theta}, m^p_{\theta\theta}, \mu^p_{\theta\theta}\}\mathrm{d}\zeta + \int_{\frac{h_e}{2}}^{\frac{h_e}{2}+h_p} \frac{\cos^2\left(\frac{\pi}{h_p}\rho\right)}{R+\zeta}\{\epsilon^p_{\theta\theta}, m^p_{\theta\theta}, \mu^p_{\theta\theta}\}\mathrm{d}\zeta,$$

$$\left\{\mathrm{N_\psi}, \mathrm{N_\phi}, \mathrm{M_\psi}, \mathrm{M_\phi}\right\} = \int_{-\frac{h_e}{2}-h_p}^{-\frac{h_e}{2}} \left\{e^p_{\theta\theta\theta}\frac{2\psi_0}{h_p}, q^p_{\theta\theta\theta}\frac{2\phi_0}{h_p}, \zeta e^p_{\theta\theta\theta}\frac{2\psi_0}{h_p}, \zeta q^p_{\theta\theta\theta}\frac{2\phi_0}{h_p}\right\}\mathrm{d}\zeta + \int_{\frac{h_e}{2}}^{\frac{h_e}{2}+h_p} \left\{e^p_{\theta\theta\theta}\frac{2\psi_0}{h_p}, q^p_{\theta\theta\theta}\frac{2\phi_0}{h_p}, \zeta e^p_{\theta\theta\theta}\frac{2\psi_0}{h_p}, \zeta q^p_{\theta\theta\theta}\frac{2\phi_0}{h_p}\right\}\mathrm{d}\zeta,$$

$$\left\{\mathrm{D_\psi}, \mathrm{D_\phi}, \mathrm{B_\psi}, \mathrm{B_\phi}\right\} = \int_{-\frac{h_e}{2}-h_p}^{-\frac{h_e}{2}} (R+\zeta)\frac{\pi}{h_p}\sin\left(\frac{\pi}{h_p}\rho\right)\left\{\frac{2\psi_0}{h_p}\epsilon^p_{rr}, \frac{2\phi_0}{h_p}m^p_{rr}, \frac{2\psi_0}{h_p}m^p_{rr}, \frac{2\phi_0}{h_p}\mu^p_{rr}\right\}\mathrm{d}\zeta + \int_{\frac{h_e}{2}}^{\frac{h_e}{2}+h_p} (R+\zeta)\frac{\pi}{h_p}\sin\left(\frac{\pi}{h_p}\rho\right)\left\{\frac{2\psi_0}{h_p}\epsilon^p_{rr}, \frac{2\phi_0}{h_p}m^p_{rr}, \frac{2\psi_0}{h_p}m^p_{rr}, \frac{2\phi_0}{h_p}\mu^p_{rr}\right\}\mathrm{d}\zeta.$$